High-K structure in ^{77}As

J. Döring, G. D. Johns, R. A. Kaye, K. W. Kemper, H. Sun,* G. N. Sylvan, and S. L. Tabor
Department of Physics, Florida State University, Tallahassee, Florida 32306

(Received 23 January 1996)

High-spin states in ^{77}As have been studied via the ^{76}Ge$(\alpha,p2n)$ reaction. Proton-gated excitation functions extracted from measured γ-ray yields at beam energies of 32, 36, and 40 MeV and an additional γ-γ coincidence measurement at 40 MeV have been used to assign new γ-ray decay sequences to ^{77}As. In particular, a positive-parity sequence up to spin $\frac{25}{2}$ and a high-lying $\Delta I=1$ sequence up to $\frac{21}{2}$ and of probably negative parity have been found to decay into the known $\frac{9}{2}^+$ isomer at 475.5 keV. Nuclear-shape calculations show a triaxial shape for the positive-parity states with moderate quadrupole deformation. The high-lying negative-parity sequence is interpreted as a high-K three-quasiparticle band similar to bands in adjacent nuclei. [S0556-2813(96)00206-3]

PACS number(s): 21.10.Re, 23.20.Lv, 25.55.Hp, 27.50.+e

I. INTRODUCTION

The presence of $\frac{9}{2}^+$ isomers in the odd-A As isotopes is well known. Their excitation energies decrease from 1422 keV in ^{67}As [1] to 304 keV in ^{75}As [2,3], followed by a slight increase to 475 keV in ^{77}As [2,4] and to 773 keV in ^{79}As [5]. Low-lying $\frac{5}{2}^+$ states are also known from β-decay work in most of the odd-mass As isotopes. The occurrence of these low-lying $\frac{9}{2}^+-\frac{5}{2}^+$ doublet states in the level spectra of ^{75,77}As could be fairly well explained in the framework of the Coriolis-coupling model with a pairing interaction at prolate deformation [6,7]. In these calculations the positive-parity states have been found to be highly mixed. For prolate deformation the decoupling of the $K^\pi=\frac{1}{2}^+$ band together with the strong Coriolis interactions between bands based on states originating from the $g_{9/2}$ proton subshell shifts the high-spin states down in energy, accounting for the observed level structure satisfactorily. Furthermore, $\frac{13}{2}^+$ states are expected in ^{75,77}As at about 750 keV above the $\frac{9}{2}^+$ isomer for a quadrupole deformation of $\beta\approx0.10$–0.15 (see Fig. 5 in Ref. [6]). However, in both nuclei these high-spin states have not yet been seen experimentally. The observation of low-lying $\frac{1}{2}^+$ states [7] in some of the odd-mass As isotopes has been taken as additional support for the Coriolis-coupling model, and a somewhat higher prolate deformation ($\beta=+0.2$) has been suggested, leading to a calculated energy for the $\frac{13}{2}^+$ state of about 560 keV above the $\frac{9}{2}^+$ state.

As a consequence of these model considerations, high-spin bands feeding into the isomer are expected to occur in the neutron-rich ^{75,77}As isotopes. However, experimental data for such high-spin decay sequences are known only for the neutron-deficient $^{67-73}$As isotopes which can easily be produced via heavy-ion reactions. From properties of these decay sequences and the energy of the $\frac{9}{2}^+$ isomer, a slight increase in the quadrupole deformation can be deduced with increasing neutron number (from $N=34$ in ^{67}As to $N=40$ in ^{73}As), with a possible maximum around the $N=42$ nucleus ^{75}As. However, experimental studies extending the in-beam data systematics to the neutron-rich isotopes have not yet been performed, possibly due to the small cross sections expected for producing these isotopes. The present work reports the results of an in-beam study of ^{77}As using α-particle beams to populate moderate and high-spin states.

Furthermore, in several of the $N=44$ isotones, e.g., ^{79}Br [8], ^{81}Rb [9], and ^{83}Y [10], high-lying three-quasiparticle (3qp) states have been found to be connected by fast $M1$ transitions [$B(M1)\approx0.5$ Weisskopf units (W.u.)] with almost no $E2$ crossover transitions (except for ^{83}Y). These $\Delta I=1$ bands start at spin $\frac{13}{2}^-$ in ^{79}Br, $\frac{13}{2}^-$ in ^{81}Rb, and $\frac{17}{2}^-$ in ^{83}Y and, hence, exhibit a high-K quantum number ($K\approx\frac{11}{2}$ or $\frac{13}{2}$). Therefore, a second goal of the present study was to search for a similar high-K band structure in the $N=44$ nucleus ^{77}As. A comprehensive compilation of the experimental data about 3qp structures in the mass 80 region can be found in Ref. [11].

So far, only low-spin states (including the $\frac{9}{2}^+$ isomer) are known in ^{77}As from previous investigations, in particular from (^{3}He,d) [12,13] and (d,^{3}He) [14] reaction studies and from β^--decay investigations [2,4,15,16]. The lifetime and g factor of the first excited $\frac{5}{2}^-$ state at 264.4 keV have also been measured [17].

II. EXPERIMENTAL TECHNIQUES AND RESULTS

States in ^{77}As have been populated using the ^{76}Ge$(\alpha,p2n)^{77}$As reaction at 32, 36, and 40 MeV beam energy. The α-particle beams were provided by the FN Tandem-superconducting LINAC facility at Florida State University. They were produced in a specially designed source where a small amount of He$^+$ was converted to He$^-$ in a metastable state which is long enough lived ($\approx$0.5 ms) to bring it to the high-voltage Tandem terminal. After stripping and further acceleration in the Tandem, the He^{2+} beam was postaccelerated by the superconducting LINAC to achieve the final energies of 32, 36, or 40 MeV. Two different in-beam experiments have been carried out: (i) a charged particle-γ-ray coincidence experiment for identification of transitions associated with ^{77}As and (ii) a γ-γ

*Permanent address: Department of Physics, Jilin University, Changchun, Jilin 130023, People's Republic of China.

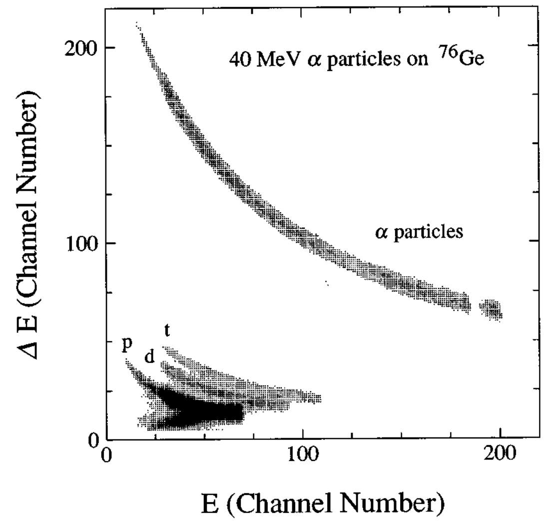

FIG. 1. Charged particle ΔE-E matrix measured with a Si detector telescope placed at 45° during the irradiation of a thin ^{76}Ge target with 40 MeV α particles. The number of counts is proportional to the grayness which is plotted in a square-root scale to enhance the weak reaction channels. The symbols p,d, and t mark proton, deuteron, and triton events, respectively.

prompt coincidence experiment for establishing the level scheme. In both experiments the target was a self-supporting foil with a thickness of about 500 μg/cm^2 enriched to 94.6% in ^{76}Ge. The strongest target contaminations were ^{72,74}Ge with 1.7% and 2.3%, respectively.

A. Particle-gated γ-ray excitation functions

To search for prompt γ rays depopulating excited states in ^{77}As, a charged-particle–γ-ray coincidence experiment has been carried out at 32, 36, and 40 MeV beam energies. The charged particles were recorded with two ΔE-E telescopes placed at 45° in the forward direction at about 2 cm distance from the target. Each telescope consisted of two Si detectors, a 75 μm ΔE and a 1000 μm E counter. The sensitive detector area was about 50 mm^2 for each telescope. Evaporated protons up to about 12 MeV and α particles up to about 50 MeV were completely stopped in the E counters. Protons with higher energies gave smaller E signals again. A relevant particle ΔE-E matrix measured with one of the telescopes at 40 MeV beam energy is shown in Fig. 1. The evaporated protons and α particles are well separated. A small number of evaporated deuterons and tritons has been recorded as well.

During the experiment the γ rays were recorded with six Compton-suppressed high-purity Ge detectors and a low-energy photon spectrometer (LEPS). Four Ge detectors and the LEPS were placed at 90° and two Ge detectors were in backward direction at 145° relative to the beam axis. The Ge detectors and the LEPS were operated in prompt coincidence with the two particle telescopes. Both types of prompt coincidence events, charged-particle–γ and γ-γ events, were selected by the data acquisition system, digitized, and written on 8 mm tape for off-line analysis. In addition, time information from LEPS events in coincidence with charged particles was also stored on tape. For this purpose, a time-to-

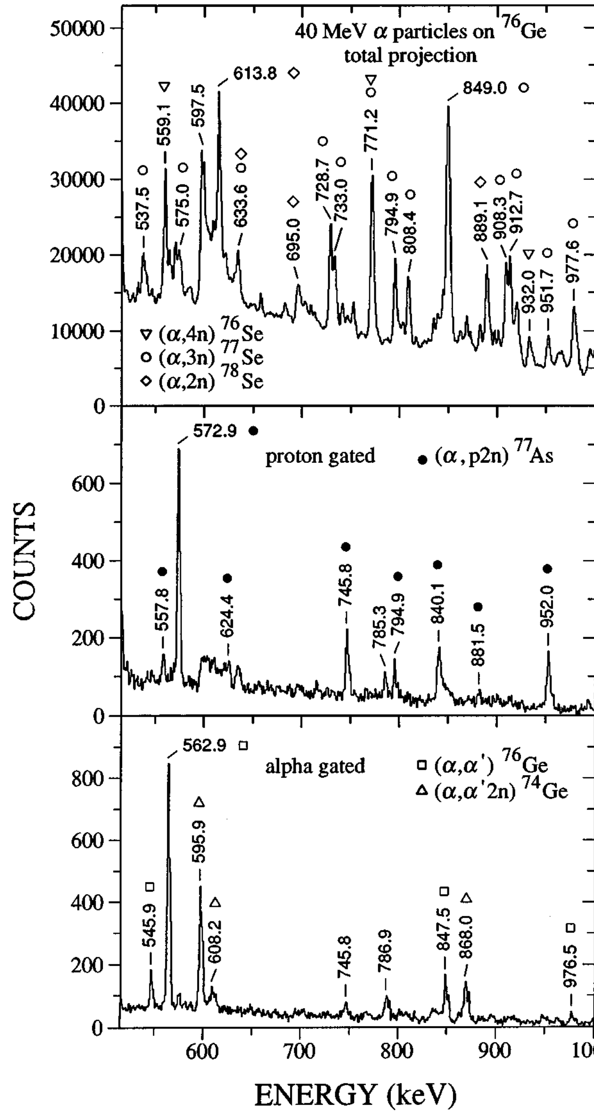

FIG. 2. Gamma-ray spectra recorded during the bombardment of a thin ^{76}Ge target with 40 MeV α particles. The top spectrum shows the total γ-ray projection of all twofold coincidence events including γ-γ and charged-particle–γ coincidences. In the middle and bottom panels, the γ rays in prompt coincidence with protons and α particles, respectively, are displayed. The spectra from both Si telescopes have been added together.

amplitude converter was started by the LEPS time signal and stopped by the delayed signal of the particle telescope being fired. For energy and efficiency calibrations radioactive sources of ^{133}Ba and ^{152}Eu have been used.

Proton and α-particle-gated γ-ray spectra have been sorted off line. Examples are given in Fig. 2 from the data set measured at 40 MeV beam energy. At this energy, most of the γ rays produced originate from the pure neutron evaporation channels, the strongest being the ^{76}Ge$(\alpha,3n)$^{77}Se reaction. The relative cross sections calculated by PACE2, a modified version of a statistical model program for heavy-ion reactions [18], for the $(\alpha,3n)$ and the $(\alpha,p2n)$ reactions are 77% and 3%, respectively. The remaining 20% of the reaction strength leads mainly to the even-even ^{76,78}Se, the odd-odd ^{78}As, and to some Ge isotopes via the $(\alpha,\alpha' xn)$ reactions. The expected production of ^{77}As nuclei is quite weak but within the detection limits of the setup.

The γ-ray spectrum (middle panel of Fig. 2) in prompt coincidence with protons at 40 MeV beam energy shows several transitions, e.g., 572.9, 745.8, and 952.0 keV lines, which we firmly assign to the odd-mass ^{77}As nucleus produced via the $(\alpha,p2n)$ reaction. For comparison the total coincidence spectrum (top panel in Fig. 2) and the α-particle-gated spectrum (bottom panel of Fig. 2) are also shown. Some strong and well-known transitions have been labeled. The identification of ^{77}As lines is also supported by the fact that most of the new γ rays do not show any prompt coincidences with these well-known lines in ^{76,77,78}Se. Furthermore, other assignment possibilities like a twofold proton reaction channel, can be excluded since two-proton–γ coincidences at this relatively low beam energy were not observed.

It has been possible to distinguish between the $(\alpha,pn)\,^{78}$As and $(\alpha,p2n)\,^{77}$As reactions from proton-gated excitation functions of the γ rays involved. In particular, several low-energy transitions, e.g., 128, 153, and 184 keV, have been newly assigned to the odd-odd nucleus ^{78}As [19]. They form their own level scheme typical for an odd-odd nucleus and do not show coincidence relationships with the transitions associated with ^{77}As, except for a 258 keV line which is a close-lying doublet.

A few examples of relative excitation functions deduced from experimental γ-ray intensities are shown in Figs. 3(b) and 3(c). They can be compared with relative excitation functions calculated with PACE2 as shown in panel (a). The PACE2 results have been renormalized to obtain a constant distribution for the ^{78}Se yield. In the same way all experimental intensities have been renormalized. The normalization factors have been obtained assuming a flat distribution for the $4^+\rightarrow2^+$ 889 keV transition in ^{78}Se. This line is not affected by the β^- decay of ^{78}As and is almost a pure single line in the measured spectra. There is a fair agreement in the slopes between the calculated and experimental excitation functions given in panels (a) and (b). The obvious difference in the total production yields between ^{77}Se and ^{78}Se can be attributed to the fact that not all of the ground-state transitions in ^{77}Se are considered, but only the $\frac{13}{2}^+\rightarrow\frac{9}{2}^+$ 849 keV line.

In addition, some relative excitation functions of lines in ^{77}As are shown in Fig. 3(c). Here the 572.9 keV line has been used for normalization. The different slopes of the excitation functions support the spin assignments discussed later, in particular that the transitions in the new positive-parity sequence, e.g., 572.9, 952.0, and 1150.6 keV, depopulate levels with increasing spin.

Furthermore, γ rays produced via the $(\alpha,\alpha' xn)^{74,76}$Ge reactions have clearly been identified as can be seen in the bottom panel of Fig. 2. The low-lying levels of the even-even ^{74,76}Ge nuclei are well known from β-decay studies [20,21]. The γ-ray energies observed in our experiment are in fair agreement with compiled data. Also, the calculated and experimental excitation functions obtained for the 597 keV line in ^{74}Ge (see Fig. 3) are in fair agreement.

B. Thin-target γ-γ coincidence experiment

A standard γ-γ coincidence experiment has been performed at 40 MeV beam energy to establish the level scheme of ^{77}As. The same ^{76}Ge target as in the charged-particle–γ-ray coincidence experiment was employed. For part of the coincidence experiment, a stack of two such targets was used as well.

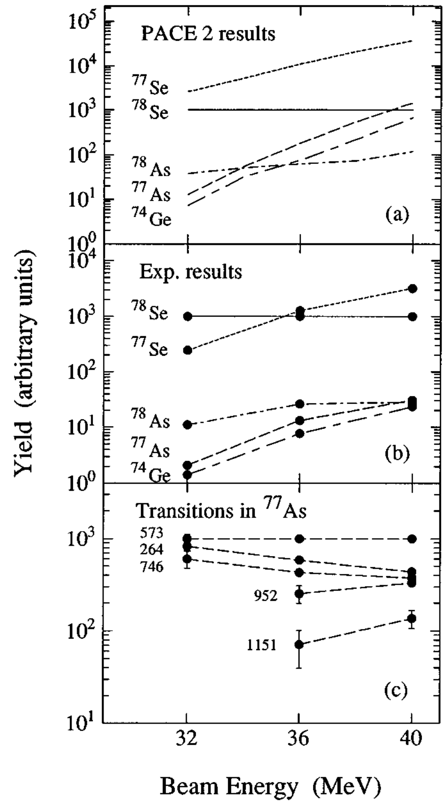

FIG. 3. Relative excitation functions obtained for the bombardment of α particles on a ^{76}Ge target. The top panel (a) shows renormalized results of PACE2 calculations. The middle panel (b) displays experimental results for different reaction channels deduced from the measured γ-ray intensities. In the case of ^{77,78}As and ^{74}Ge, particle-gated γ-ray intensities have been used. For relative normalization the measured intensity of the $4^+\rightarrow2^+$ 889 keV transition in ^{78}Se has been set to 1000 and all other measured intensities renormalized accordingly. For the different channels the following lines have been displayed: ^{77}Se, 849 keV; ^{78}As, 184 keV; ^{77}As, 573 keV; ^{74}Ge, 597 keV. In the bottom panel (c) the proton-gated excitation functions for several new transitions in ^{77}As are shown. Here the intensity of the 573 keV has been taken for normalization.

The emitted γ rays were detected with the Pittsburgh-Florida State Universities detector array [22] consisting at the time of eight high-purity Ge detectors of about 25% relative efficiency surrounded by bismuth-germanate $Bi_4Ge_3O_{12}$ (BGO) anti-Compton shields. The BGO multiplicity filter was not used since emphasis was placed on low-multiplicity events. The Ge detectors were placed about 18 cm from the target, four detectors at 90° and four detectors at a backward angle of 145° relative to the direction of the beam.

The data were stored on 8 mm tape and sorted off line into a triangular matrix with a dispersion of 0.8 keV per channel. This matrix contained about 15×10^6 coincidence events. Energy and efficiency calibrations were made using a ^{152}Eu source. The energy calibration of each detector was checked and readjusted using precise energies known from

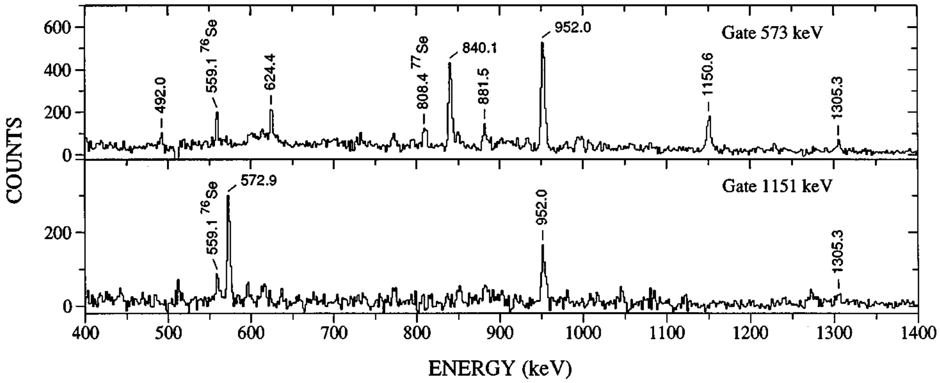

FIG. 4. Portions of background-corrected coincidence spectra generated by gating on the 573 and 1151 keV transitions in the total prompt triangular matrix.

(n,γ) reactions for transitions in ^{77}Se [23] and ^{76}Se [24].

For constructing the ^{77}As level scheme, gates were set in the triangular matrix on the peaks of interest with appropriate background corrections, i.e., by subtracting a background gate set near the line of interest. A few examples of gated coincidence spectra relevant for the new structures are given in Figs. 4 and 5. Figure 4 shows the transitions in the positive-parity sequence. A narrow gate has been set on the 573 keV transition, to avoid contaminations from the 569 and 574 keV transitions of ^{77}Se. The results for the ^{77}Se nucleus will be presented elsewhere [25]. Figure 5 illustrates coincidences from the high-lying level structure via the 160.3 keV decay path. The new $\Delta I=1$ transitions at 160.3, 257.5, 360.9, and 492.0 keV can be seen clearly. It should be mentioned that the high-lying 257.5 keV transition forms a close-lying doublet with a γ ray newly assigned to ^{78}As [19] produced in our measurement via the (α,pn) reaction.

For spin assignments using directional correlation of oriented nuclei (DCO) ratios, the measured data were also sorted into a square matrix where the events from the 90° detectors were sorted against the events from the backward detectors. DCO ratios of γ rays have been extracted from this matrix according to the equation

$$R_{\mathrm{DCO}}=\frac{I_{\gamma}(\text{at } 145°\text{gated by}\gamma_G \text{ at } 90°)}{I_{\gamma}(\text{at } 90°\text{gated by}\gamma_G \text{ at } 145°)}, \qquad (1)$$

where I_γ is the observed intensity of the transition of interest and γ_G is the gating transition. When the gate is a stretched $E2$ transition, the ratio is expected to be close to unity for a $\Delta I=2$ transition and close to 0.5 for a stretched $\Delta I=1$ transition. These predictions have been successfully verified for well-known $E2$ and $M1$ transitions in ^{76,77,78}Se. Wherever possible from the counting statistics, gates were also set on transitions in ^{77}As to deduce DCO ratios. Since no stretched $E2$ transitions were known prior to this work, individual R_{DCO} values extracted from different gating transitions are compiled in Table I. Here, $\Delta I=1$ transitions have also been used as gates in order to gather as much information as possible about transitions in ^{77}As. If the DCO ratio of the gating $\Delta I=1$ transition is close to 0.5, DCO ratios of 1 and 2 will be obtained for stretched $\Delta I=1$ and 2 transitions, respectively.

A cross check of the DCO matrix has been performed for low-energy γ transitions to verify that the detector efficiencies in our setup have been taken properly into account and that there is no significant energy dependence of the DCO ratios. For this purpose, the γ rays involved in the decay of the $\frac{9}{2}^{+}$ isomer of ^{77}As, the 211.1 and 264.4 keV transitions, have been analyzed with respect to DCO ratios, too. They show DCO ratios close to unity in the 265 and 211 keV gates, respectively, as expected since the original alignment is completely attenuated due to the long isomeric half-life of 114 μs.

On the basis of the experimental excitation functions, available DCO ratios and observed decay pattern, spin, and parities for the states in ^{77}As have been deduced. They are compiled in Table I together with the transition energies and intensities.

III. LEVEL SCHEME OF ^{77}As

The new level scheme extracted from the present measurements is given in Fig. 6. As already pointed out, a decay

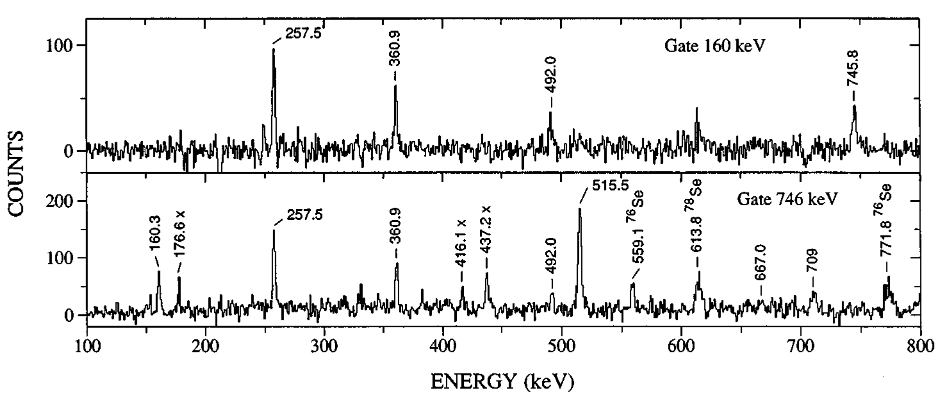

FIG. 5. Portions of background-corrected coincidence spectra generated by gating on the 160 and 746 keV transitions in the total prompt triangular matrix. Peaks labeled with the letter x have not been assigned.

TABLE I. Energy, intensity, asymmetry ratios, and multipolarity for transitions assigned to ^{77}As as well as spin, parity, and energy of the initial state.

E_γ [a] (keV)	I_γ [b]	R_{DCO} [c] (573 keV)	R_{DCO} [c] (258 keV)	R_{DCO} [c] (264 keV) or (746 keV)	σL [d]	I_π [e]	E_{level} (keV)
160.3(2)	5(1)		1.03(14)		$(M1)$	$\frac{15}{2}^{(-)}$	2745.3
211.1(1)				1.01(3)	$M2$ [f]	$\frac{9}{2}^{+}$ [f]	475.5
215.5(2)	14(1)				$M1/E2$ [f]	$\frac{3}{2}^{-}$ [f]	215.5
257.5(2)	10(2)	0.57(8)		1.09(23)	$(M1)$	$\frac{17}{2}^{(-)}$	3002.8
264.4(1)	43(2)				$M1/E2$ [f]	$\frac{5}{2}^{-}$ [f]	264.4
360.9(2)	7(2)	0.55(5)	0.98(11)	0.94(21)	$(M1)$	$\frac{19}{2}^{(-)}$	3363.7
367.6(2)	≈2			1.61(26)	$(E1)$ [f]	$\frac{5}{2}^{(+)}$ [f]	632.0
416.6(3)	≈3				$(E1)$ [f]	$\frac{5}{2}^{(+)}$ [f]	632.0
492.0(2)	5(1)	0.52(7)			$(M1)$	$\frac{21}{2}^{(-)}$	3855.7
515.5(2)	20(4)			1.03(9)	$(M1/E2)$	$\frac{13}{2}^{(+)}$	1736.8
557.8(2)	8(2)				$E1$ [f]	$\frac{7}{2}^{-}$ [f]	1189.8
572.9(2)	100(4) [g]	1.08(10) [h]			$E2$	$\frac{13}{2}^{+}$	1048.4
624.4(2)	≈6						2512.9
625.1(3)	≈2						889.5
667.0(4)	≈2				$(E2)$	$\frac{15}{2}^{+}$	1888.5
674.1(4)	≈2						889.5
709(1)	≈2						1929.9
745.8(2)	36(3)		0.91(10)		$M1/E2$	$\frac{11}{2}^{+}$	1221.3
794.9(2)	12(1)			2.22(21)	$E2$	$\frac{9}{2}^{-}$	1059.3
840.1(2)	28(3)	0.36(6)			$M1/E2$	$\frac{15}{2}^{+}$	1888.5
881.5(3)	5(2)						1929.9
952.0(2)	33(3)	0.94(8)			$E2$	$\frac{17}{2}^{+}$	2000.4
1008.4(5)	5(3)				$(E1)$	$\frac{15}{2}^{(-)}$	2745.3
1065(1)	≈2						2124
1150.6(3)	11(3)	1.10(17)			$E2$	$\frac{21}{2}^{+}$	3151.0
1305.3(5)	4(2)	1.16(21) [i]			$E2$	$\frac{25}{2}^{+}$	4456.3
1363.8(5)	4(2)				$(E1)$	$\frac{13}{2}^{(-)}$	2585.0
1696.9(6)	6(3)	0.44(12)			$(E1)$	$\frac{15}{2}^{(-)}$	2745.3

[a]Uncertainty in the last digit is given in parentheses.
[b]Intensity determined from the proton-gated γ-ray spectrum at 40 MeV. In case of doublets, the coincidence relations have been taken into account.
[c]DCO ratio determined from the gate given in parentheses.
[d]Multipolarity.
[e]Spin of the initial state.
[f]Spin and parity assignments to the isomer and some low-lying levels as well as the multipolarities of the transitions observed in their decay have been adopted from Refs. [2,4,15,16].
[g]Normalization.
[h]Value deduced from the 952 keV gate.
[i]Value deduced from the sum of 573, 952, and 1151 keV gates.

sequence consisting of 572.9, 952.0, 1150.6, and 1305.3 keV γ rays has been found in our data set which is in prompt coincidence with evaporated protons. In addition, this sequence does not show any coincidence relationships with known transitions in ^{76,77,78}Se.

The new sequence has been placed on top of the $\frac{9}{2}^{+}$ isomer at 475.5 keV since the excitation functions point to rather high-spin states. Spin assignments are deduced from the measured DCO ratios which are close to 1.0 for all four transitions, hence giving evidence for the $\Delta I=2$ nature of these transitions. The $E2$ multipolarity of these transitions is obvious from their prompt coincidence relations; i.e., the transitions are fast and not nanoseconds delayed so that an $M2$ character can be excluded. (An assumed $M2$ transition probability of 1 W.u. corresponds to a lifetime of about 40 ns for the 572.9 keV transition.) Increasing spin is evident from the experimental excitation functions, and positive parity is also supported by similarities with decay sequences feeding the $\frac{9}{2}^{+}$ isomers in adjacent nuclei, e.g., ^{71,73}As [26,27] and ^{79}Br [8]. Thus, states with $\frac{13}{2}^{+}$, $\frac{17}{2}^{+}$, $\frac{21}{2}^{+}$, and $\frac{25}{2}^{+}$ have been identified in ^{77}As for the first time.

Another sequence of γ rays at 257.5, 360.9, and 492.0 keV has been found to be in coincidence with the 572.9 keV transition via a linking 1696.9 keV γ ray. These γ rays establish levels at 2745.3, 3002.8, 3363.7, and 3855.7 keV. An independent decay path of the 2745.3 keV level via the

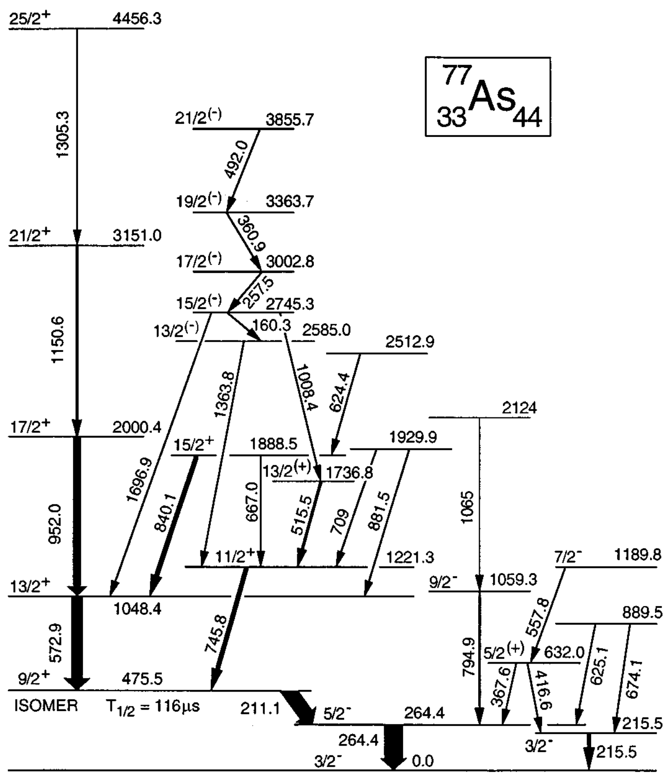

FIG. 6. Level scheme of ^{77}As as deduced from the present experiment. Spin and parity assignments for the $\frac{9}{2}^+$ isomer and a few low-lying levels have been taken from Refs. [2,4,15,16].

160.3, 1363.8, and 745.8 keV transitions supports the placement of the high-lying level structure. At the same time, the 745.8 keV transition establishes the 1221.3 keV $\frac{11}{2}^+$ state. The ordering of the 745.8 and 1363.8 keV transitions is fixed by the observation of a 515.5 keV γ ray not seen in the 1363.8 keV coincidence gate. Therefore, the 515.5 keV line establishes a level at 1736.8 keV. This level is fed by a 1008.4 keV transition, depopulating the 2745.3 keV state.

A search has been made to find transitions linking the new high-lying level structure to the lower-lying negative-parity states, as they were seen in ^{79}Br or ^{81}Rb. However, no firm connection could be found.

It should be mentioned that in the β^- decay [4] of the $\frac{7}{2}^+$ ground state of ^{77}Ge to ^{77}As, a weak 745.75 keV transition has been observed feeding into the $\frac{9}{2}^+$ isomer. However, no spin and parity assignments had previously been proposed to the initial level at 1221.21 keV. Our assignment of $I^\pi = \frac{11}{2}^+$ to this level is compatible with the β^- decay data where the weak decay to the 1221.21 keV level (no log ft value given in Ref. [4]) is a second forbidden transition with no parity change. The 1221.3 and 1888.5 keV states appear to be signature partners to the main positive-parity sequence. However, positive parity for the 1736.8 keV level is not as certain.

The DCO ratios for the 257.5, 360.9, 492.0, and 1696.9 keV transitions have been deduced from the 572.9 keV gate, resulting in values close to 0.5 (see Table I). This points to $\Delta I = 1$ transitions. Also in the $\Delta I = 1$ 258 keV gate, the DCO ratios deduced for the depopulating transitions are close to 1.0 suggesting $\Delta I = 1$ character for the lines at 160.3 and 745.8 keV. All these DCO values support the proposed spin values. Negative parity of the high-lying structure is tentatively proposed based on systematics.

A prompt coincidence gate set on the known low-lying 264.4 keV transition in ^{77}As revealed, in addition to some other γ rays, transitions of 794.9 and 1065 keV. The 794.9 keV line shows a DCO ratio of about 2.22(21) in the $\Delta I = 1$ 264.4 keV gate, suggesting a stretched $\Delta I = 2$ character. On the other hand, the 264.4 keV transition shows a DCO ratio of 0.45(5) in the 794.9 keV gate compatible with the known $\frac{5}{2}^- \rightarrow \frac{3}{2}^-$ nature of this transition. These findings extend the negative-parity states up to 2124 keV in excitation energy with the level at 1059.3 keV having spin and parity of $\frac{9}{2}^-$.

In the β^- decay compilation [4], a 794.33 keV transition has been observed in coincidence with the 264.4 keV transition. For the initial level at 1058.74 keV, a spin of $\frac{3}{2}^-$ had been assigned based on the log ft value of 10.28. In addition, the extracted proton transfer angular momentum of $l_p = 1$ for a level observed at 1052(5) keV in the (^{3}He,d) reaction [13] and at 1052(6) keV in the (d, ^{3}He) reaction [14] was used to back up this spin and parity assignment. However, the population of the 1059.3 keV level in the present experiment does not support such a low spin, and the energy difference of about 7 keV compared to the reaction data suggests that there are two different levels, at 1052 and 1059.3 keV. The known log ft value would also agree with a spin and parity assignment of $\frac{9}{2}^-$, as proposed from our in-beam data. Furthermore, the assignment of positive parity to the $\frac{5}{2}$ state at 632.0 keV based on a log ft = 7.699 value in the β^- decay [4] looks unlikely for an allowed β transition.

IV. DISCUSSION

A. Positive-parity states

Previously, the observation of low-lying states of $\frac{1}{2}^+$, $\frac{5}{2}^+$, and $\frac{9}{2}^+$ and their theoretical understanding in the framework of the rotational model with strong Coriolis coupling provided early evidence for the occurrence of moderate prolate-deformed nuclei in this mass region [6,7]. However, the model prediction of highly mixed states of $\frac{11}{2}^+$ and $\frac{13}{2}^+$ originating from the $g_{9/2}$ proton subshell with less than 1 MeV excitation energy above the $\frac{9}{2}^+$ isomer has, so far, not been verified in ^{77}As. Now, the experimental excitation energy of these states at 572.9 and 745.8 keV above the isomer provides additional support for the assumption of a static quadrupole deformation in the As isotopes. The energy of the $\frac{13}{2}^+ \rightarrow \frac{9}{2}^+$ transition of 572.9 keV is still smaller than in ^{73}As (610 keV) and comparable with the corresponding transition energy (589 keV) in the isotone ^{79}Br. In all these nuclei the positive-parity bands have been associated with a $g_{9/2}$ proton excitation. Thus, the same configuration is proposed for the new band in ^{77}As. The moments of inertia for the positive-parity band in ^{77}As and those of ^{79}Br are shown in Fig. 7. The similarities are quite obvious. In both nuclei the dynamic moment of inertia, $J^{(2)}$, rises with increasing rotational frequency $\hbar\omega$. Unfortunately, the bands are not known to high enough spins to see the first upbend or backbend. Systematics predict some collectivity for these states in ^{77}As, as in ^{79}Br, which we cannot verify due to the lack of lifetime measurements.

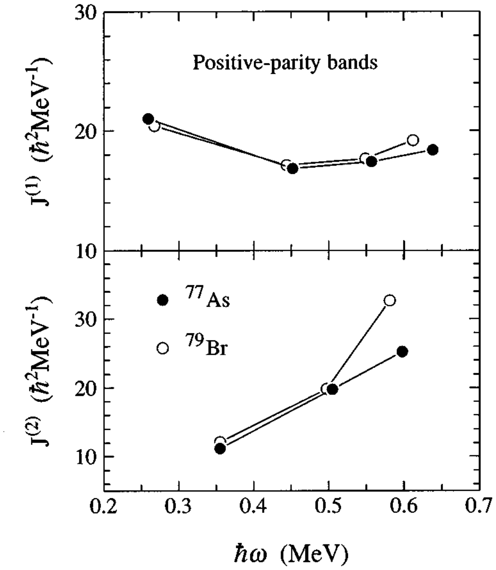

FIG. 7. Kinematic, $J^{(1)}$, and dynamic, $J^{(2)}$, moments of inertia for the positive-parity sequences built on the $\frac{9}{2}^+$ isomers in ^{77}As and ^{79}Br. A value of $K=\frac{5}{2}$ has been taken for both bands.

B. Three-quasiparticle states

The high-lying level structure with tentatively assigned negative parity in ^{77}As shows intense $\Delta I=1$ transitions and energy spacings like the known $\Delta I=1$ 3qp bands in ^{79}Br and ^{81}Rb. A more detailed comparison of the level energies among these $N=44$ isotones is given in Fig. 8. With decreasing proton number from $Z=37$ in ^{81}Rb to $Z=33$ in ^{77}As the 3qp levels are shifted up slightly in energy. Also, the level spacings increase slightly. Furthermore, the decay of the lowest states is somewhat different. Whereas in ^{81}Rb and ^{79}Br the decay happens to both positive- and negative-parity low-lying states, in ^{77}As only the decay to the positive-parity states by a few high-energy transitions has been found. The similarities in energy spacings are remarkable, suggesting similar internal high-K structures with $K\approx\frac{11}{2}$ or $\frac{13}{2}$. In ^{79}Br and ^{81}Rb, a 3qp configuration was proposed where an unpaired $g_{9/2}$ proton is coupled to a broken neutron pair; one neutron is lifted to the intruder $g_{9/2}$ subshell and the other one occupies the negative-parity $p_{1/2}$, $p_{3/2}$, and/or $f_{5/2}$ subshells. The same 3qp configuration is now proposed for the high-lying structure in ^{77}As.

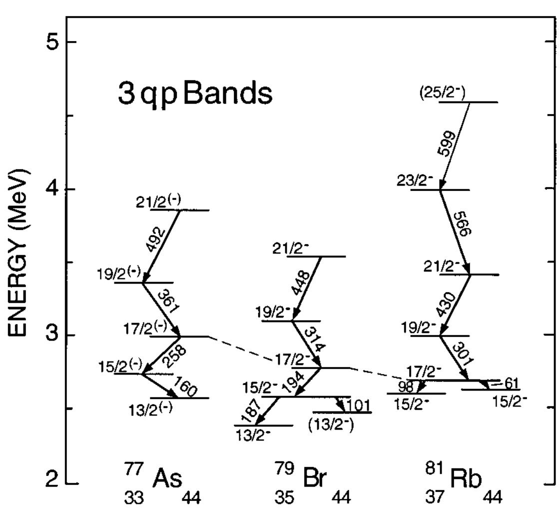

FIG. 8. Comparison of level energies for the high-lying negative-parity states in the $N=44$ isotones ^{77}As, ^{79}Br, and ^{81}Rb. The experimental data have been taken from ^{79}Br [8] and ^{81}Rb [9].

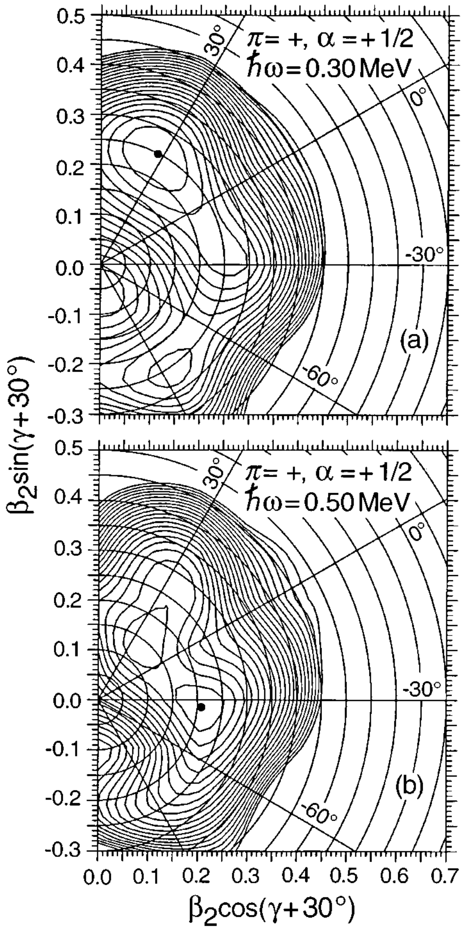

FIG. 9. Total Routhian surfaces calculated in the (β_2,γ) plane using the model of Ref. [30] for positive-parity states with signature $\alpha=+\frac{1}{2}$. The odd proton is assumed to occupy the $g_{9/2}$ subshell. Panels (a) and (b) show the results for 0.30 and 0.50 MeV rotational frequency, respectively. Prolate- and oblate-deformed shapes rotating collectively correspond to triaxiality parameters $\gamma=0°$ and $-60°$, respectively.

It should be mentioned that shell-model calculations have been performed recently for a similar high-lying $\Delta I=1$ band in the $N=48$ nucleus ^{85}Rb, where the level energies and $M1$ transition probabilities could be reproduced fairly well on the basis of a three-particle-hole excitation of the type $\pi g_{9/2}^{1}\otimes\nu g_{9/2}^{-1}\otimes\nu f_{5/2}^{-1}$ [28].

C. Shape calculations for ^{77}As

The nuclear ground-state deformation of ^{77}As has been calculated with a macroscopic-microscopic model [29] resulting in an electric quadrupole moment of $Q_2=1.0$ b. Assuming an axially deformed shape this would correspond to a deformation of $\beta_2=0.146$ which is typical for the so-called transitional region close to the line of stability.

The shape evolution of ^{77}As as a function of the rotational frequency has been studied using the Hartree-Fock-Bogolyubov formalism [30]. Total Routhian surfaces (TRS's) have been calculated for ^{77}As for different rotational frequencies and different single-particle configurations. A few results are shown in Fig. 9 for positive-parity states where the odd proton occupies the $g_{9/2}$ subshell, a situation underlying the experimentally observed positive-parity sequence. The results show moderate quadrupole deformation of about $|\beta_2| \approx 0.25$ with a triaxiality of $\gamma \approx +32°$ for a low rotational frequency. With increasing frequency, the shape changes to a smaller quadrupole deformation with a triaxiality of $\gamma \approx -31°$, i.e., to a shape with the ability of collective rotation.

V. SUMMARY

In summary, high-spin states in ^{77}As built on the $\frac{9}{2}^+$ isomer have firmly been identified up to $\frac{25}{2}^+$ and $\frac{21}{2}^{(-)}$ using charged-particle–γ and γ-γ coincidence measurements via the ^{76}Ge$(\alpha,p2n)$ reaction at 32, 36, and 40 MeV beam energy. The new positive-parity sequence on top of the $\frac{9}{2}^+$ isomer at 475.5 keV is described as a $g_{9/2}$ proton excitation, while a high-lying decay sequence consisting of intense $\Delta I=1$ transitions is interpreted, based on similarities in energy spacings with bands in ^{79}Br and ^{81}Rb, as a negative-parity 3qp band predominantly containing the $\pi g_{9/2} \otimes \nu g_{9/2} \otimes \nu(p_{1/2}, p_{3/2}, f_{5/2})$ configuration.

ACKNOWLEDGMENTS

The authors thank Dr. J.X. Saladin for the loan of the University of Pittsburgh Ge detectors used for the combined Pitt-FSU detector array. We would also like to thank Dr. R. Wyss and Dr. W. Nazarewicz for providing the TRS computer codes. This work was supported in part by the U.S. National Science Foundation and the State of Florida.

[1] T.F. Lang, D.M. Moltz, J.E. Reiff, J.C. Batchelder, J. Cerny, J.D. Robertson, and C.W. Beausang, Phys. Rev. C **42**, R1175 (1990).

[2] A.W. Schardt, Phys. Rev. **108**, 398 (1957).

[3] A.R. Farhan and S. Rab, Nucl. Data Sheets **60**, 735 (1990).

[4] A.R. Farhan, S. Rab, and B. Singh, Nucl. Data Sheets **57**, 223 (1989).

[5] B. Singh, Nucl. Data Sheets **70**, 437 (1993).

[6] W. Scholz and F.B. Malik, Phys. Rev. **176**, 1355 (1968).

[7] R.R. Betts, D.J. Pullen, W. Scholz, and B. Rosner, Phys. Rev. Lett. **26**, 1576 (1971).

[8] R. Schwengner, J. Döring, L. Funke, H. Rotter, G. Winter, A. Johnson, and A. Nilsson, Nucl. Phys. **A486**, 43 (1988).

[9] J. Döring, R. Schwengner, L. Funke, H. Rotter, G. Winter, B. Cederwall, F. Lidén, A. Johnson, A. Atac, J. Nyberg, and G. Sletten, Phys. Rev. C **50**, 1845 (1994).

[10] T.D. Johnson, F. Cristancho, C.J. Gross, M. Kabadiyski, K.P. Lieb, D. Rudolph, M. Weiszflog, T. Burkardt, J. Eberth, and S. Skoda, Z. Phys. A **347**, 285 (1994) and references quoted therein.

[11] S.L. Tabor and J. Döring, Phys. Scr. T **56**, 175 (1995).

[12] R.R. Betts, S. Mordechai, D.J. Pullen, B. Rosner, and W. Scholz, Nucl. Phys. **A230**, 235 (1974).

[13] M. Schrader, H. Reiss, G. Rosner, and H.V. Klapdor, Nucl. Phys. **A263**, 193 (1976).

[14] G. Rotbard, M. Vergnes, J. Vernotte, G. Berrier-Ronsin, J. Kalifa, and R. Tamisier, Nucl. Phys. **A401**, 41 (1983).

[15] R.D. Meeker and A.B. Tucker, Nucl. Phys. **A157**, 337 (1970).

[16] R.N. Cherry, Jr. and M.L. Wiedenbeck, Nucl. Phys. **A252**, 445 (1975).

[17] M. Mohsen and F. Pleiter, Nucl. Phys. **A500**, 277 (1989).

[18] A. Gavron, Phys. Rev. C **21**, 230 (1980).

[19] J. Döring , G. D. Johns, D. J. Hartley, R. A. Kaye, K. W. Kemper, G. N. Sylvan, and S. L. Tabor, Z. Phys. A **354**, 345 (1996).

[20] A.R. Farhan, Nucl. Data Sheets **74**, 529 (1995).

[21] B. Singh, Nucl. Data Sheets **74**, 63 (1995).

[22] S.L. Tabor, M.A. Riley, J. Döring, P.D. Cottle, R. Books, T. Glasmacher, J.W. Holcomb, J. Hutchins, G.D. Johns, T.D. Johnson, T. Petters, O. Tekyi-Mensah, P.C. Womble, L. Wright, and J.X. Saladin, Nucl. Instrum. Methods Phys. Res. B **79**, 821 (1993).

[23] Y. Tokunaga, H. Seyfarth, R.A. Meyer, O.W.B. Schult, H.G. Börner, G. Barreau, H.R. Faust, K. Schreckenbach, S. Brant, V. Paar, M. Vouk, and D. Vretenar, Nucl. Phys. **A439**, 427 (1985).

[24] Y. Tokunaga, H. Seyfarth, O.W.B. Schult, H.G. Börner, Ch. Hofmeyr, G. Barreau, R. Brissot, U. Kaup, and Ch. Mönkemeyer, Nucl. Phys. **A411**, 209 (1983).

[25] G.D. Johns *et al.* (unpublished).

[26] R.S. Zighelboim, S.G. Buccino, F.E. Durham, J. Döring, P.D. Cottle, J.W. Holcomb, T.D. Johnson, S.L. Tabor, and P.C. Womble, Phys. Rev. C **50**, 716 (1994).

[27] B. Heits, H.-G. Friederichs, A. Rademacher, K.O. Zell, P. von Brentano, and C. Protop, Phys. Rev. C **15**, 1742 (1977).

[28] R. Schwengner, G. Winter, J. Reif, H. Prade, L. Käubler, R. Wirowski, N. Nicolay, S. Albers, S. Esser, P. von Brentano, and W. Andrejtscheff, Nucl. Phys. **A584**, 159 (1995).

[29] P. Möller and J.R. Nix, At. Data Nucl. Data Tables **26**, 165 (1981).

[30] W. Nazarewicz, J. Dudek, R. Bengtsson, T. Bengtsson, and I. Ragnarsson, Nucl. Phys. **A435**, 397 (1985).